EVOLUTIONARY BIOLOGY

The evolution of anti-bat sensory illusions in moths

Juliette J. Rubin[1]*†, Chris A. Hamilton[2]*†, Chris J. W. McClure[1,3], Brad A. Chadwell[4], Akito Y. Kawahara[2]*‡, Jesse R. Barber[1]*‡

Prey transmit sensory illusions to redirect predatory strikes, creating a discrepancy between what a predator perceives and reality. We use the acoustic arms race between bats and moths to investigate the evolution and function of a sensory illusion. The spinning hindwing tails of silk moths (Saturniidae) divert bat attack by reflecting sonar to create a misleading echoic target. We characterized geometric morphometrics of moth hindwings across silk moths, mapped these traits onto a new, robust phylogeny, and found that elaborated hindwing structures have converged on four adaptive shape peaks. To test the mechanism underlying these anti-bat traits, we pit bats against three species of silk moths with experimentally altered hindwings that created a representative gradient of ancestral and extant hindwing shapes. High-speed videography of battles reveals that moths with longer hindwings and tails more successfully divert bat attack. We postulate that sensory illusions are widespread and are underappreciated drivers of diversity across systems.

INTRODUCTION

One driver of life's diversity is the imperative for prey under attack to overpower, outrun, or redirect their assailants (*1*, *2*). To divert predatory strikes, prey can manipulate predator perception (*3*). Sensory illusions selected to misdirect attack target the primary sensory systems of predators to distort prey-related information (*4*, *5*). Traits that create sensory illusions are common throughout life: Large, mimetic eyespots on butterfly wings and fish fins deflect and deter visual predators (*6*–*8*); sea hares eject ink that their chemosensory-oriented predators often pursue as alternative prey (*9*). Traits that create similar sensory illusions repeatedly originate across unrelated groups, likely driven by the intense selective pressure of predation and the constraints of effectively transmitting an illusion to the chief sensory channel of a predator: Eyespots occur across insects [for example, butterflies, beetles, grasshoppers, and katydids (*10*, *11*)] and vertebrates [for example, fish, birds, and frogs (*12*)]; cuttlefish, squid, and octopus produce ink secretions with equivalent chemical profiles to those of sea hares (*13*). Sensory illusions can thus elucidate intimate evolutionary relationships between prey and predators (*14*), as well as potentially common flaws in the processing of each sensory system (*15*). Here, we investigate how silk moth (Saturniidae) diversification might be explained by evolutionary exploration of vulnerabilities in the auditory system of bats.

The bat-moth arms race has escalated along an acoustic channel and is an ideal system to use the power of the Tinbergian model (*16*) to understand sensory illusions by simultaneously investigating both evolutionary history and the underlying mechanism. For millions of years, moths have navigated the nightly threat of their echolocating predators (*17*). Recent work with wild silk moths (Saturniidae) indicates that spinning hindwing tails divert bat attack toward these expendable structures, away from the vital body core (*18*). These dynamic trailing appendages create an echoic sensory illusion, reflecting bat sonar in a manner that distracts from the body target or displaces the echoic target center (*19*, *20*).

[1]Boise State University, Boise, ID 83725, USA. [2]The McGuire Center for Lepidoptera and Biodiversity, University of Florida, Gainesville, FL 32611, USA. [3]The Peregrine Fund, Boise, ID 83709, USA. [4]Idaho College of Osteopathic Medicine, Meridian, ID 83642, USA.
*Corresponding author. Email: julietterubin@boisestate.edu (J.J.R.); chamilton@flmnh.ufl.edu (C.A.H.); kawahara@flmnh.ufl.edu (A.Y.K.); jessebarber@boisestate.edu (J.R.B.)
†These authors contributed equally to this work.
‡These authors are co-principal investigators.

An initial investigation using a five-gene–based phylogeny demonstrated that twisted and cupped tails evolved multiple times on different continents across the family [*Copiopteryx* (Arsenurinae), South America; *Eudaemonia* (Saturniinae), Africa; and *Actias* and *Coscinocera* (Saturniinae), Asia (fig. S1) (*18*)]. Furthermore, this early work indicated that tail length might increase after origination. Here, we pursue the proximate and ultimate causes of hindwing traits in moths (*16*). We predict that specific wing shapes evolved in silk moths to misconstrue information encoded in returning echoes to bats. To probe the adaptive shape space of silk moth hindwings, we used more advanced phylogenetic techniques combined with morphometric analyses and found emergent, distinct shape regimes. We experimentally recreated these by altering the hindwings of live moths and then pit the resulting morphs against bat predators to test their relative survival success in bat-moth battles. By these means, we track how ancient predatory pressure has molded prey into extant forms, equipped to foil the very sensory systems that hound them.

RESULTS AND DISCUSSION

To more strenuously examine the evolution of hindwing traits and diversification within Saturniidae, we used a phylogenomic data set of 797 loci (*21*). Rather than a gradual, transitional history of increasing hindwing length and complexity, we see abrupt shifts in shape across phylogeny (Fig. 1). Moreover, trait-dependent diversification analysis (*22*) indicates that having a hindwing projection of any length is associated with increased diversification rates in the lineage (see Materials and Methods). Geometric morphometrics and tests of convergence reveal that hindwings occupy at least four adaptive shape space regimes (Fig. 2A), independent of phylogenetic relationships. These adaptive peaks are broadly defined as extra long–tailed (statistically split into distinct adaptive peaks, occupying similar morphospace; Fig. 1, regimes 1 and 2), short-tailed (regime 3), and long-lobed (regime 4) (movies S1 to S4). Hindwing shape is likely more available to evolutionary modification from pressures other than flight, compared to forewing shape (*23*), due to decreased flight constraints. A study testing the relative roles of Lepidoptera wings found that complete removal of the hindwings primarily limits maneuverability, while forewing removal renders the animal flightless (*24*). Thus, although strikes to a moth hindwing can be costly, structural damage to the forewing could be deadly.

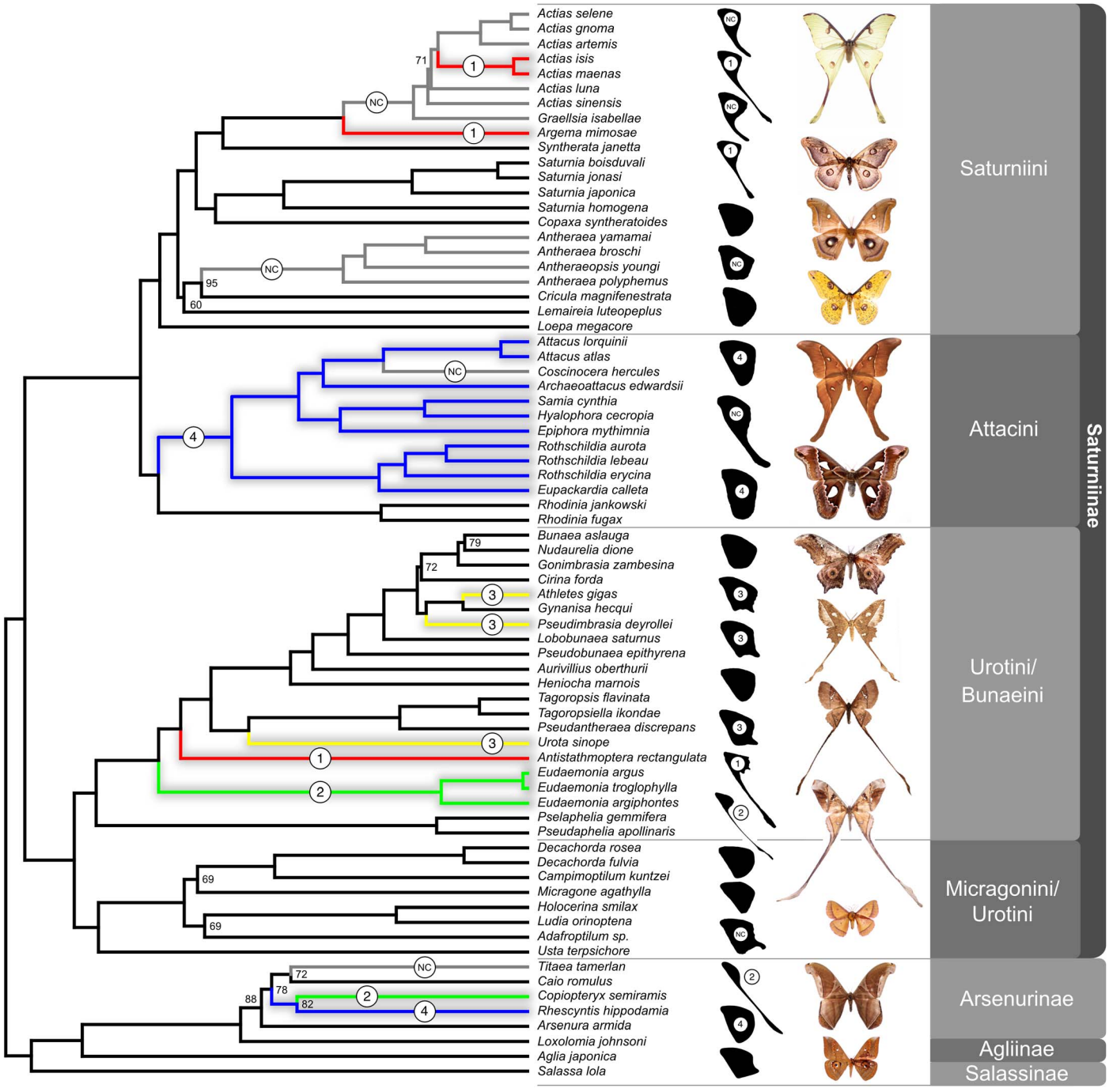

Fig. 1. Maximum likelihood tree of Saturniidae shows that elongated hindwing lobes and hindwing tails convergently evolved multiple times. Colored branches indicate the four identified convergent regimes and adaptive peaks, denoted by a white numerical circle. Regimes 1 and 2 (red and green, respectively), extra long tail; regime 3 (yellow), short tail; regime 4 (blue), elongated lobes. Gray branches labeled NC indicate nonconvergent adaptive peaks. Phylogeny based on 797 anchored hybrid enrichment (AHE) loci; all nodes are supported by 100% bootstrap values unless otherwise noted.

To test the anti-bat efficacy of these convergent hindwing shapes, we pit 16 big brown bats (*Eptesicus fuscus*) against moths with experimentally altered hindwings (fig. S2) from the Saturniidae subfamily Saturniinae, a diverse clade comprising more than 1300 extant tailed and tailless species. Geometric morphometric analysis of our experimentally altered moths indicates that these treatments fall realistically within the morphospace tracked by extant subfamilies and were therefore effective recapitulations of silk moth morphology (Fig. 2B). We recorded bat-moth battles in a dark, foam-lined flight room using multiple synchronized, spatially calibrated, high-speed cameras and ultrasonic microphones trained on an interaction space defined by the flight range of a moth tethered to a 1-m monofilament line. From these behavioral results,

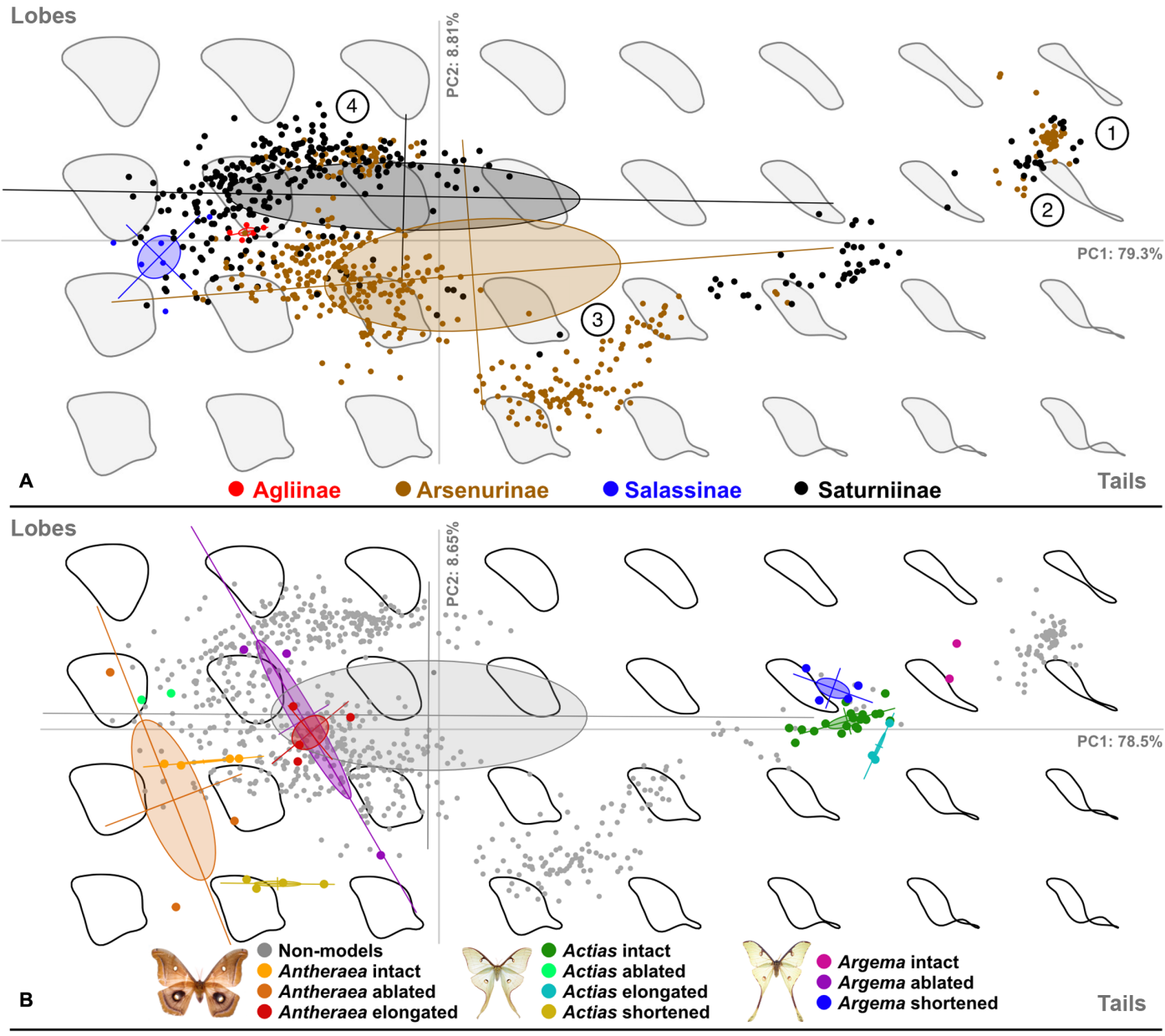

Fig. 2. Geometric morphometric analysis of hindwing shape reveals changes in morphospace across four saturniid subfamilies. Principal components analyses (PCA) visualize hindwing morphospace by (**A**) subfamily, showing that Saturniinae and Arsenurinae have independently evolved into the same morphospace. PC, principal component. (**B**) Experimental treatment, showing that moths with hindwing alterations exist in similar morphospace to extant species that have not been subjected to wing alteration. Dots represent individual specimens in the analysis. Color refers to (A) subfamily or (B) experimental manipulations. Confidence ellipses facilitate understanding of shape space and the amount of variation residing within subfamilies. Hypothetical shape approximations are plotted in the background to aid in visualizing shape change. In addition, the four identified convergent regimes and adaptive peaks, seen in Fig. 1, are denoted by a white numerical circle. Regimes 1 and 2, extra long tails; regime 3, short tails; and regime 4, elongated hindwing lobes.

we infer the role of enlarged hindwing lobes (that is, uniform elongated hindwing area) and twisted and cupped hindwing tails across Saturniidae.

To quantify the antipredator role of the elongated lobe adaptive peak (Fig. 1, regime 4), we simulated shortened and enlarged hindwing lobe conditions in the naturally tailless polyphemus moth (*Antheraea polyphemus*) by cutting and/or gluing hindwing material (fig. S2). We assessed the anti-bat efficacy of hindwing morphology using Bayesian models, including moth size as a covariate, individual bat identity as random intercepts, and bat experience (that is, number of nights hunting moths) as random slopes to focus our analysis on the outcome of bat-moth battles. Polyphemus moths with experimentally enlarged hindwing lobes, akin to wing shapes found in the Attacini tribe (Fig. 1), escape bat attack more often than moths without enhancement [hindwing length elongated = 5.8 ± 0.40 cm (means ± SD), escape success = 56 ± 0.11%; hindwing length intact = 5.4 ± 0.29 cm, escape success = 27 ± 0.09%] (Fig. 3, *n* for each treatment listed in the figure legend). While we found no difference in escape success between polyphemus with experimentally shortened hindwing area (hindwing length

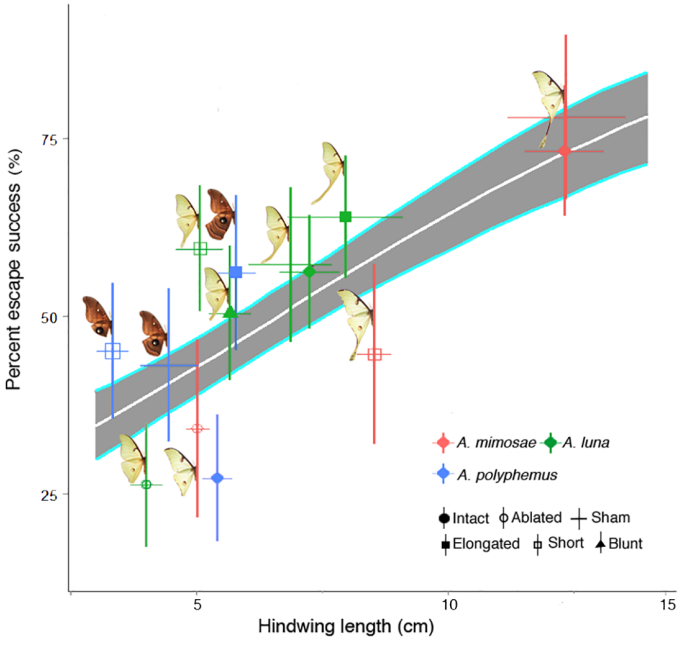

Fig. 3. Moths with longer hindwings escape an increasing proportion of bat attacks. The inner white line represents the predicted mean posterior probability distribution from a Bayesian mixed logistic regression model. The gray area is the SD of posterior probability distributions of the prediction. Points represent proportions for each treatment calculated using a Bayesian mixed logistic model controlling for bat identity and hunting night (time). Vertical bars represent the SD of posterior probability distributions, whereas horizontal error bars represent observed SD of hindwing length for each treatment. Images of moth treatments are positioned on their respective vertical error bars. Only one picture is shown for an intact or sham treatment, as they have the same morphology. Sample sizes for bat-moth interactions are as follows: *Argema mimosae* (intact = 30, ablated = 17, sham = 13, and short = 22), *Actias luna* (intact = 64, ablated = 38, sham = 37, elongated = 83, short = 93, and blunt = 48), *Antheraea polyphemus* (intact = 40, sham = 35, elongated = 29, and shortened = 44).

shortened = 3.34 ± 0.32 cm, escape success = 45 ± 0.10%) and intact polyphemus moths (27 ± 0.09%), a review of multiple high-speed camera angles of each interaction reveals that bats direct more strikes toward the hindwings of longer lobed moths (proportion of strikes toward posterior region of elongated polyphemus = 50 ± 0.11%) than the other two treatments (intact = 17 ± 0.08%, shortened = 12 ± 0.05%) (Fig. 4A and movie S5). We thus find evidence that elongated hindwing lobes increase the effectiveness of this defensive strategy and support for the convergent, adaptive peak of elongated hindwing lobes found in the Attacini and Arsenurinae (Fig. 1).

To examine the repeated convergence of long tails in Saturniidae, we tested the anti-bat advantage of different grades of tail length. We experimentally varied tail length in two species, the luna moth (*Actias luna*, tail length = 7.26 ± 0.59 cm) and the African moon moth (*Argema mimosae*, tail length = 12.32 ± 0.77 cm) (fig. S2) and pit these treatments against the same big brown bats. With complete removal of tails, escape success was low (ablated luna escape success = 26 ± 0.09%, hindwing length = 4.0 ± 0.32 cm; ablated moon moth escape success = 34 ± 0.13%, hindwing length = 5.04 ± 0.23 cm) (Fig. 3), and bats infrequently aimed their attacks at moth hindwings (proportion of posterior attacks on ablated luna = 17 ± 0.07%, ablated moon moth = 18 ± 0.10%) (Fig. 4A). We created short-tailed luna (tail length = 5.09 ± 0.47 cm) and moon moths (tail length = 8.55 ± 0.34 cm) by removing the tail shafts and regluing the twisted cupped ends to the hindwing. Intact moon moths escape bat attack far more than short-tailed or ablated morphs (intact escape success = 73 ± 0.09%, short-tailed = 45 ± 0.13%, and ablated = 34 ± 0.13%) (Fig. 3). Luna moths had more incremental variations in escape success between treatments yet track the same positive trend as the overall models, where escape success (total escape model slope = 0.18 ± 0.05) (Fig. 3) and diversion of bat attack (total posterior aim model slope = 0.31 ± 0.05) (Fig. 4A) increase with hindwing length. Despite the impressive effect of intact moon moth tails, the overall escape trend remains the same when moon moths are removed from the model (escape model slope with luna and polyphemus only = 0.17 ± 0.06). Thus, long hindwing tails provide a powerful anti-bat advantage.

Cutting and gluing hindwing material did not in itself change proficiency at evading attacking bats. Control sham treatments, with hindwing area or tails cut and reglued, yielded the same escape success (sham polyphemus = 43 ± 0.11%, sham luna = 57 ± 0.11%, and sham moon moth = 78 ± 0.12%) and drew the same proportion of bat attacks to the hindwing region (sham polyphemus = 18 ± 0.08%, sham luna = 41 ± 0.11%, and sham moon moth = 61 ± 0.14%) as intact animals of each genus. The experimental procedure also did not alter flight behavior. Three-dimensional (3D) kinematic analyses derived from synchronized, spatially calibrated, high-speed videography of intact and sham moths in flight revealed no difference in mean speed, tangential acceleration, angular velocity, or their correlated counterparts (mean curvature, radial acceleration, and tortuosity; n = 8 to 12 per treatment). Reducing and elongating the hindwing material also did not affect flight kinematics (n = 10 to 13), except in short-tailed moon moths, which had a greater mean angular velocity [turning rate sensu (*25*)] than intact moon moths (table S1). Previous studies report that increased angular velocity is positively correlated with prey escape success (*25*, *26*). However, our Bayesian model revealed no correlation between mean angular velocity and escape success and no change in overall model slope. We therefore excluded angular velocity from our models and do not attribute evasion differences between treatments to the hindwing modification methods or to flight parameters in the resulting morphs. We do not dismiss the importance of hindwing morphology for flight, however, and we note that the interaction between flight and wing shape requires future exploration, particularly in wild bat-moth interactions.

During pursuit, tails could alter bat perception of the echoic target of a moth (*18*), either via an illusion of larger size (*19*), due to an integration of echoes reflected across the moth's length with an echoic target center shifted from the moth's true center (*20*), or via the creation of two or more alternative targets induced by primary reflections from the forewings and the twisted and cupped tail ends (Fig. 4B). If tails create an illusion of larger size, then we might expect bats to attack the center of the enlarged echoic target, just behind the abdomen (movie S6) (*20*). We reviewed video footage of each interaction from three to four high-speed cameras encircling the interaction space and found that bats hunting tailed moths targeted either the body or the twisted and cupped ends of tails 75% of the time (attacks directed at moth body = 47%, attacks directed at tail ends = 28%; Fig. 4B and movie S7), while the region just behind the abdomen drew only 25% of bat strikes, far less than would be expected if hindwing tails were shifting the apparent center of the moth to this post-abdominal region. Together, these data support an illusion of multiple targets. A similar alternative target illusion also exists in the visual system, when bird attacks are drawn from the head and anterior wing margins of butterflies (*27*) to deceptive "false heads" twitching at the tips of the butterflies' hindwings (*28*, *29*).

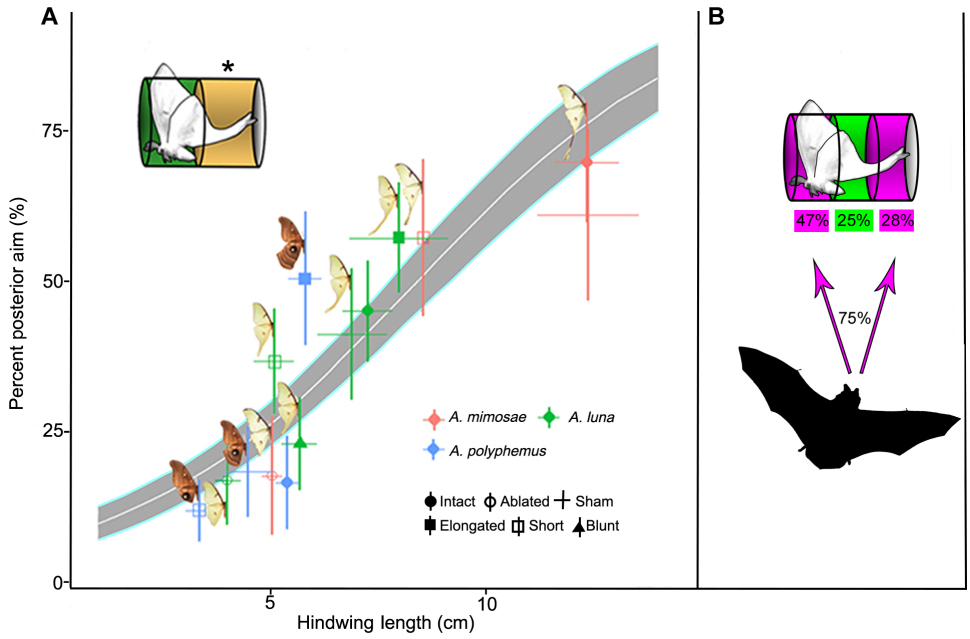

Fig. 4. Hindwing tails redirect bat attack against moths. Behavioral analyses reveal that (**A**) bats aim an increasing proportion of their attacks at the posterior half of the moth (indicated by yellow cylinder with asterisk) and that (**B**) bats attacked the first and third sections of tailed moths 75% of the time [*A. luna*: intact, sham, elongated; *A. mimosae*: intact, sham, shortened (sections highlighted in purple)], providing support for the multiple-target illusion. An enlarged echo illusion would likely lead bats to target the hindwing just behind the abdomen of the moth, at the perceived echo center (second section, highlighted in green); however, bats targeted this region only 25% of the time. Bat success in capturing moths varied as they targeted different sections of the moth: first = 76%, second = 15%, and third = 6%. The model in (A) was built the same as in Fig. 3.

To begin to understand the morphology underlying tails' diversionary effect, we removed the twisted and cupped ends of luna tails, creating a blunt-tailed morph. These blunt ends exist naturally in butterflies and day-flying moths with short, unstructured tails (*30*). Blunt luna and shortened luna provide a good comparison because the length of the hindwing is similar, but shortened luna maintains the end structure (blunt-tailed length = 5.67 ± 0.42 cm, short-tailed length = 5.09 ± 0.47 cm). Both morphs escaped bat attack (blunt-tailed = 50 ± 0.10%, short-tailed = 60 ± 0.09%) (Fig. 3) and diverted bat aim to the posterior region (blunt-tailed = 23 ± 0.08%, short-tailed = 37 ± 0.09%) at roughly the same rate (Fig. 4A), whereas intact luna moths possessing longer tails with twisted and cupped ends were more successful at diverting bat attack to the hindwing region than blunt luna (intact = 45 ± 0.08%, blunt-tailed = 23 ± 0.08%). This difference is not solely reliant on tail length, however, since there is no measurable difference in the proportion of posterior attacks between intact luna and shortened luna (intact = 45 ± 0.08%, shortened = 37 ± 0.09%), despite intact luna having longer tails. Thus, the efficacy of the illusion relies to a certain degree on the twisted and cupped end of the tail.

How elaborated hindwings create an acoustic illusion likely depends on the sonar strategy and physiological limitations of the attacking bat. Moths face a diversity of bat species and echolocation types on a given night (*31*). Definitively determining the illusion created by rotating hindwing tails awaits phylogenetically widespread, multiangle ensonification experiments using a variety of sonar regimes to generate a 3D reconstruction of the perceived moth shape from all possible attack angles. Tailed moths clearly challenged the processing abilities of the frequency-modulated (FM) *E. fuscus* bats we pit them against. Over months of hunting nights, bat strike accuracy and capture success did not improve (table S2). In addition, we found no difference in bat sonar behavior across moth treatments (figs. S3 and S4 and table S3). FM bats are known to elongate the duration of their terminal sonar phases (buzz I and buzz II) when confronted with a more difficult predatory task (*32*); however, we did not observe any changes in buzz duration over time, indicating that the bats in our study did not perceive a task difficulty gradient among the moth morphs we presented (table S3).

Bats experienced the same difficulty capturing moths with experimentally elongated lobing as moths with similar length tails (Fig. 3). Tails might provide a comparable deflective effect to elongated lobing but offer less material for an attacking bat to grab during aerobatic capture maneuvers. In contrast to lobing, tails might also reduce energetic requirements for the moth during pupal development (*33*) or, perhaps more likely, provide a flight benefit, shedding air vortices during flight to improve maneuverability (*34*, *35*), although the added weight and possible drag of a tail could also have energetic costs (*36*). Our kinematic assessments did not reveal differences in flight ability between tailed (luna or moon moth) and nontailed (polyphemus moth) genera (table S1) and, therefore, do not support a flight performance cost or benefit to tails, but this question deserves more study. Tails might have alternatively evolved as ornamentation for sexual selection, although wild silk moths are short-lived and females tend to mate with the first male that approaches (*37*). We would therefore predict that any sexual selection pressures are secondary to the intense natural selection imposed by bats that we quantify here.

Using phylogenetic, morphometric, and behavioral methods, we examined the evolutionary and mechanistic significance of an acoustic sensory illusion and found that bat predation drives the convergence of hindwing shape in silk moths. Physical constraints on moth wing architecture (*38*) and physiological and cognitive restrictions of echolocation processing in bats (*39*) together seem to propel silk moth

hindwing shape to distinct, convergent morphological regimes, with hindwing extensions accelerating diversification rates within lineages. Our data indicate that the evolutionary path of possible shape space in moth hindwings is hedged by the ability of these forms to transmit credible sensory illusions through the acoustic channel. Given their efficacy, echoic illusions generated by elaborated wing structures may be a common anti-bat strategy that spans insect families and life histories. Twisted and cupped hindwing tails have evolved in at least three other families of Lepidoptera (Himantopteridae, Sematuriidae, and Uraniidae) and in Nemopteridae (spoonwings) (*40*). Further studies are needed to determine whether each of these iterations produces the same illusion based on sonar strategy and angle of bat attack. We propose that illusions targeting specific predator sensory systems are powerful drivers of convergent evolution across life, and the outcomes of these predator-prey interactions likely significantly influence speciation and extinction (*41*).

MATERIALS AND METHODS

Experimental animals

We used 16 adult female *E. fuscus* bats mistnetted in Idaho between 2015 and 2016 and maintained in a clock-shifted animal housing room (dark, 9 a.m. to 5 p.m.), kept at 24° to 27°C and >40% humidity. Vertebrate work was done following Boise State University's Animal Care and Use Committee protocol (number 006-AC14-018). We kept bats in captivity for a total of 3 to 13 months and did not use them for experimental trials during the winter months (November to April). Before beginning trials, we gave all bats an acclimation period of 2 to 4 weeks in the laboratory. After completion of experiments, we released bats at the site of capture. To maintain physical conditions, we flew each bat individually daily, regardless of whether she was participating in trials that day. We fed bats one to two mealworms coated in Missing Link or Vionate Powder nutritional supplements to augment their daily diet and provided water ad libidum. Bats that did not catch and successfully eat the one to two silk moths and two small pyralid "control" moths (*Galleria mellonella*) presented during experimental trials were fed five to nine extra mealworms to supplement their caloric needs.

We reared silk moth pupae at the McGuire Center for Lepidoptera and Biodiversity at the University of Florida and allowed them to eclose at Boise State University. To encourage efficient eclosion, we kept them under constant light conditions, with an ambient 24° to 27°C environment and humidity >75%. We pit moths against bats within 3 days of eclosion and did not handle them until that point.

Geometric morphometrics, phylogenomics, ancestral state reconstruction, and convergence analysis

We conducted geometric morphometric analysis of 804 natural history collection specimens, mapped across a phylogenomic data set of 797 loci. We first measured shape variation among silk moth hindwings using elliptical Fourier descriptor (EFD) analysis in the R program *Momocs* (*42*) to place pseudo-landmarks around a closed outline (that is, hindwing shape) and eliminate size as a variable. The first harmonic was used to normalize the harmonic coefficients and make them invariant to size and rotation. This approach allows quantifiable analysis of shape when there are few or no identifiable homologous landmarks (*42*–*46*). EFD uses the first ellipse to normalize for rotation, translation, size, and orientation and then uses harmonic coefficients for subsequent statistical analysis, PCA, and visualization.

To investigate how morphological space is occupied across Saturniidae, we digitized male specimens from four closely related saturniid subfamilies: Arsenurinae, Agliinae, Saturniinae, and Salassinae. Previous phylogenetic work reveals that, although closely related, these subfamilies are not sister lineages (*47*). Arsenurinae and Saturniinae contain species with hindwing lobes and tails, while Agliinae and Salassinae do not. Thus, the elaborated hindwing traits that we find in Arsenurinae and Saturniinae most likely emerged from separate origination events. We used Photoshop or Affinity Photo to highlight, cut, and smooth hindwing shapes. We chose male specimens because females of many species are not represented in museum collections. We also digitized 23 images of experimentally altered specimens from the bat-moth trials to determine whether the experimental shapes fell within biologically similar and realistic morphospace. Within *Momocs*, we defined outlines as the closed polygon formed by the (x, y) coordinates of bounding pixels. We used the "calibrate_harmonics" function to evaluate the number of harmonics needed to effectively describe the shapes in this analysis, without overparameterization, and found that 99% of the power was captured when the number of harmonics was set at nb.h = 12. We included both the elliptical Fourier coefficients and computed PC outputs in subsequent comparative analyses.

To establish our new phylogenomic data set, we followed the pipeline of Breinholt *et al.* (*21*) to clean, assemble, and determine the orthology of AHE loci (*48*). We used MAFFT v7.245 to execute multiple sequence alignments (*49*). After excluding loci with more than 50% missing data, we kept 797 loci (193,048 base pairs in total) for 73 silk moth species for inclusion in the study. We assembled a concatenated supermatrix using FASconCAT-G v1.02 (*50*) and included species from the subfamilies Agliinae, Arsenurinae, and Salassinae to confirm the relationships of these closely related subfamilies and to highlight that the Saturniinae and Arsenurinae are not direct sister lineages. We carried out phylogenetic inference using IQ-TREE MPI multicore v1.5.3 (*51*), and individual site models of evolution were determined in IQ-TREE using Bayesian information criterion [see data files in the Dryad Digital Repository (____)].

For comparative analyses, we created a relative rate–scaled ultrametric tree using the "chronopl" function in the R package ape (*52*, *53*). We evaluated phylogenetic signal in our trait data using the R package Rphylopars (*54*). A likelihood ratio test revealed significant phylogenetic signal in the phylogenetic residuals ($P < 0.0001$) [see Revell (*55*)]. We tested for trait-dependent diversification (or state-dependent diversification) by using the nonparametric test within the R package *FiSSE* [fast, intuitive, state-dependent, speciation-extinction (*22*)] on binary characters, defined as whether a lineage had a hindwing projection. Those lineages with any hindwing projection displayed increased diversification rates ($P = 0.014$). To visualize the morphospace and investigate putative convergence events, we explored 3D phylomorphological space. Using the elliptical Fourier data and phylogeny, we corrected for evolutionary relationships using a phylogenetic PCA (pPCA) in phytools. We plotted the pPCA values [phylogenetic PCs (pPCs) 1 to 3] in phylomorphospace (movies S1 to S4) using modified code [originally from the phytools blog (blog.phytools.org) and Eberle *et al.* (*56*)] from the "phylomorphospace3d" function in phytools [see "ColoredPhylomorphospace3d_function.R" in the Supplementary Materials on the Dryad Digital Repository (___)]. To quantifiably test for convergence of hindwing morphological shape space, we used the R package SURFACE (*57*) on the first three phylogenetically corrected PCs; these three pPCs described most of the hindwing shape variation.

We identified four convergent, adaptive peaks (numbers 1 to 4 in Fig. 1 and movies S3 and S4), as well as four additional adaptive peaks that were not convergent with any other lineages in this analysis (see NC in Fig. 1). These adaptive peak designations include both tailed and non-tailed lineages. To investigate the number of times that hindwing tails, elongated hindwing lobes, and the various adaptive peaks evolved, we performed ancestral state reconstruction (ASR) on the maximum likelihood tree using the R package phytools (*58*). We simulated stochastic character mapping 10,000 times on a data set with all tips coded for type of hindwing shape morphology or SURFACE regime. Stochastic character mapping in "make.simmap" is a powerful Bayesian approach that samples a large number of possible discrete character histories, allows for changes to occur along branches, and assesses the uncertainty in character history due to topology and branch lengths (*59*). To define hindwing shape morphology character states, we applied our knowledge of Saturniidae taxonomy and hindwing morphology while using the results from the geometric morphometric analyses as a guide. Hindwing character states were broadly defined as having one of the following: an extra long tail, a long tail, a short tail, graded extensions of the hindwing (lobes), or no tail. We identified adaptive peaks (convergent or nonconvergent) in the SURFACE analysis (figs. S5 and S6 and movies S1 to S4).

Bat-moth battles

To test the anti-bat efficacy of these convergent hindwing shapes, we pit 16 big brown bats (*E. fuscus*) against moths with experimentally altered hindwings (fig. S2) that followed the shape regimes we identified on phylogeny. We altered hindwing shape by removing hindwing lobes or tails with small scissors at designated spots on the hindwing or by adding hindwing material using skin glue (see fig. S2 for complete description of each treatment). We assigned each silk moth one of several possible hindwing alteration treatments and photographed it against graph paper for size analysis before the trial began. We later measured the surface area and hindwing length of each moth from our photos using ImageJ (*60*) and included these measurements in our models as covariates to control for body size.

We recorded bat-moth battles in a dark flight room (7.6 m × 6.7 m × 3 m) lined with anechoic foam at Boise State University. Illumination was provided to researchers by two red ceiling lights and a red headlamp and to the camera array by eight infrared Wildlife Engineering LED (light-emitting diode) arrays. We filmed all interactions with three synchronized, high-speed, infrared-sensitive cameras [120 frames per second (fps), 3.5-mm lens; Basler Scout] and an additional high-speed camera (Basler Scout) fitted with a 6-mm lens to aid in behavioral assessments. We ran all cameras at 100 fps and focused the array on an area of the room defined by a 1-m monofilament line secured to the ceiling. We trained bats to approach this tether by stringing small pyralid moths (*G. mellonella*) from it during each flight session. After a 2-week post-capture acclimation period, and once a bat was consistently catching pyralid moths off the tether with 90 to 100% success, we began the experimental trials. To affix silk moths to the tether, we slid the monofilament line through the pronotum. We did not consider bats to be ready to begin experiments until they repeatedly attacked tethered silk moths.

Once a bat was ready for trials, we presented one to three silk moths per night in randomized order, commonly resulting in each bat hunting different moth species of varying treatments each night. We presented two *G. mellonella* in pseudo-randomized order, one at the beginning of the experimental night and one partway through, to ensure that bat motivation levels were high. Before allowing the bat to attack, we verified that moths were adequately flying. So long as a moth was flying normally, we would allow the bat to make multiple capture attempts on the same moth. We suspended the trial if a moth ceased flying or if it incurred wing damage. Upon review of the high-speed video recordings, we removed interactions from the data set where moths exhibited unnatural flight.

We reviewed all interactions using a custom-built LabVIEW program to visualize the three synchronized camera views and MaxTRAQ for the fourth, closeup shot. From these multiple angles, we noted the behavior type as a binary variable [capture or no capture by bat (escape), aim location, no contact (miss), and location of damage on the moth's wings, if applicable] and time stamp within the video for each interaction so that audio and video data could be analyzed together. We defined "capture" (no escape) behaviors as the bat being able to grab and carry the moth out of the interaction space. We classified "aim" as the bat's directional heading at either the forewing and body (anterior) or hindwing (posterior) of the moth three frames before the interaction. For moths with twisted and cupped tail ends [*A. luna* (intact, sham, and elongated) and *A. mimosae* (short, intact, and sham)], we included an additional aim category: cupped end. "Miss" was defined as a bat making no contact with the moth, despite exhibiting complete capture behaviors, including sonar attack behavior and aerobatic catching maneuvers (for example, closing the wing membranes as if to envelope prey). We determined the location of bat-related damage on moths by visually inspecting the video footage and post-interaction photos.

To analyze our behavioral results, we used generalized linear mixed models fit under a Bayesian framework to examine differences between treatment groups and relationships between dependent variables and tail length (*61*, *62*). We used models including treatment as a fixed factor and subtracted samples from posterior distributions of treatments to obtain posterior distributions of differences between treatments. We determined whether comparisons were different when 95% credible intervals from the resulting distribution did not intersect zero (*61*–*63*). To determine relationships with tail length, we used models that included tail length as a covariate and considered there to be a difference between comparisons if the 95% credible intervals for the posterior distribution of the slope did not intersect zero (*61*–*63*). We implemented the model in JAGS version 4.2.0 (*64*) using the jagsUI package version 1.4.4 (*65*) and R version 3.2.3 (*66*). We ran three chains for 50,000 generations, following a 10,000 generation burn-in. We used standard weakly informative priors (*62*) and visually assessed traceplots and used the Gelman-Rubin statistic (*67*) to check for convergence. We built escape and aim models with binomial distributions and logit links. In all models, we included moth surface area as a covariate to control for body size and individual bat identity and hunting night as random intercepts and slopes, respectively, to control for individual variation.

Kinematics of moth flight

We randomly selected 10 videos from each treatment for digitization, beginning 100 frames (1 s) out from the frame of bat-moth interaction. Video frame of interaction was determined either by frame of first contact or, in the case of misses, by frame when the bat completed its full capture behavior. When possible, we did not digitize an individual moth's flight path more than once, even if it contributed multiple trials to our data set. We were only able to digitize eight sham *A. mimosae* flights because of camera view obstruction (for example, moth flew behind one of the mounted microphones or the researcher's hand

obscured the flight path). Using DLTdv5 and easyWand5 packages in MATLAB (*68*, *69*), we digitized moth flight from our recorded bat-moth interactions on the tether, with the center of moth body as our focal point. We ran our outputs through a custom-built MATLAB package (written by B.A.C.) and extracted flight parameters of interest for evading predatory capture, as defined by Combes *et al.* (*25*). After running a correlation matrix [R package Hmisc (*70*)], we found that mean speed, mean tangential acceleration, and mean angular velocity were uncorrelated with each other but highly correlated (>0.7) with one or more of the other variables. We therefore limited our comparisons to include only these three parameters, which we included in Bayesian models as described above using normal distributions and identity links.

Echolocation

We recorded all attack sequences using four ultrasonic Avisoft microphones [CM16, ±3 dB (Z), 20 to 140 kHz] connected to a four-channel Avisoft UltraSoundGate 416H (sampling at 250 kHz) via XLR cables and recording to a desktop computer running Avisoft Recorder software. We synchronized audio and visual feeds by triggering both with a National Instruments 9402 digital I/O module. Three of the microphones surrounded the interaction space in triangular formation, each equidistant from the monofilament line, while the fourth perched directly above the center of the interaction space. We analyzed 10 to 15 call sequences per moth treatment, using one to two sound files from at least three different bat individuals, with Avisoft SASLab Pro software (Hann Window, 1024 fast Fourier transform). When possible, we selected one file from a bat's initial trial and one file from a trial near the end of the experiments to account for duration of experience hunting silk moths. We inspected all four audio channels, beginning 900 ms back from the selected interaction, and chose the channel with the highest signal-to-noise ratio to analyze [following Barber *et al.* (*18*)]. This selection always included sonar pulses from the approach [interpulse interval (IPI) >15 ms], buzz I (IPI ≤15 ms), and buzz II (IPI ≤6.5 ms) phases (*71*, *72*). Buzzes I and II are together considered the terminal phase of an echolocation attack sequence and provide the bat the final details of a prey animal's flight path through an increase in pulse emission rate (*72*–*74*). We analyzed these sonar data using the same statistical analyses as above.

SUPPLEMENTARY MATERIALS

Supplementary material for this article is available at http://advances.sciencemag.org/cgi/content/full/4/7/eaar7428/DC1

Fig. S1. Twisted and cupped hindwing tail ends in Saturniidae.
Fig. S2. Hindwing morphology of the three silk moth species was altered by cutting and gluing hindwing material.
Fig. S3. IPI does not change on the basis of moth treatment.
Fig. S4. IPI does not change on the basis of moth genus or hindwing length.
Fig. S5. ASR demonstrates multiple origins of the hindwing tail trait within the Saturniinae subfamily.
Fig. S6. ASR demonstrates multiple origins of adaptive peaks within the Saturniinae subfamily.
Table S1. Kinematic output results from 100 ms of tethered moth flight leading up to bat-moth interaction.
Table S2. Bat identity and experience (that is, learning) do not affect the outcome of the trial.
Table S3. Bats do not change call parameters during attack on silk moths of differing morphologies.
Movie S1. Phylomorphospace by tail regime.
Movie S2. Phylomorphospace by tail regime (no labels).
Movie S3. Phylomorphospace by adaptive peak.
Movie S4. Phylomorphospace by adaptive peak (no labels).
Movie S5. Bat attack on elongated hindwing lobes.
Movie S6. Bat attack on intact hindwing tails.
Movie S7. Bat attack on intact tail ends.

REFERENCES AND NOTES

1. M. Edmunds, *Defense in Animals: A Survey of Anti-predator Defenses* (Longman, 1974).
2. S. M. Vamosi, On the role of enemies in divergence and diversification of prey: A review and synthesis. *Can. J. Zool.* **83**, 894–910 (2005).
3. L. A. Kelley, J. L. Kelley, Animal visual illusion and confusion: The importance of a perceptual perspective. *Behav. Ecol.* **25**, 450–463 (2014).
4. M. Stevens, *Sensory Ecology, Behavior, and Evolution* (Oxford Univ. Press, ed. 1, 2013).
5. T. E. White, D. J. Kemp, Technicolour deceit: A sensory basis for the study of colour-based lures. *Anim. Behav.* **105**, 231–243 (2015).
6. S. De Bona, J. K. Valkonen, A. López-Sepulcre, J. Mappes, Predator mimicry, not conspicuousness, explains the efficacy of butterfly eyespots. *Proc. R. Soc. B* **282**, 1–7 (2015).
7. K. Kjernsmo, M. Grönholm, S. Merilaita, Adaptive constellations of protective marks: Eyespots, eye stripes and diversion of attacks by fish. *Anim. Behav.* **111**, 189–195 (2016).
8. K. Kjernsmo, S. Merilaita, Resemblance to the enemy's eyes underlies the intimidating effect of eyespots. *Am. Nat.* **190**, 594–600 (2017).
9. C. E. Kicklighter, S. Shabani, P. M. Johnson, C. D. Derby, Sea hares use novel antipredatory chemical defenses. *Curr. Biol.* **15**, 549–554 (2005).
10. M. Stevens, The role of eyespots as anti-predator mechanisms, principally demonstrated in the Lepidoptera. *Biol. Rev. Camb. Philos. Soc.* **80**, 573–588 (2005).
11. U. Kodandaramaiah, Eyespot evolution: Phylogenetic insights from *Junonia* and related butterfly genera (Nymphalidae: Junoniini). *Evol. Dev.* **11**, 489–497 (2009).
12. G. D. Ruxton, T. N. Sherratt, M. P. Speed, *Avoiding Attack: The Evolutionary Ecology of Crypsis, Warning Signals and Mimicry* (Oxford Univ. Press, 2004).
13. C. D. Derby, C. E. Kicklighter, P. M. Johnson, X. Zhang, Chemical composition of inks of diverse marine molluscs suggests convergent chemical defenses. *J. Chem. Ecol.* **33**, 1105–1113 (2007).
14. M. J. Ryan, When seeing is deceiving: A comment on Kelley and Kelley. *Behav. Ecol.* **25**, 466–467 (2014).
15. D. M. Eagleman, Visual illusions and neurobiology. *Nat. Rev. Neurosci.* **2**, 920–926 (2001).
16. N. Tinbergen, On aims and methods of ethology. *Z. Tierpsychol.* **20**, 410–433 (1963).
17. W. E. Conner, A. J. Corcoran, Sound strategies: The 65-million-year-old battle between bats and insects. *Annu. Rev. Entomol.* **57**, 21–39 (2012).
18. J. R. Barber, B. C. Leavell, A. L. Keener, J. W. Breinholt, B. A. Chadwell, C. J. W. McClure, G. M. Hill, A. Y. Kawahara, Moth tails divert bat attack: Evolution of acoustic deflection. *Proc. Natl. Acad. Sci. U.S.A.* **112**, 2812–2816 (2015).
19. D. H. Janzen, Two ways to be a tropical big moth: Santa Rosa saturniids and sphingids. *Oxford Surv. Evol. Biol.* **1**, 85–140 (1984).
20. W.-J. Lee, C. F. Moss, Can the elongated hindwing tails of fluttering moths serve as false sonar targets to divert bat attacks? *J. Acoust. Soc. Am.* **139**, 2579–2588 (2016).
21. J. W. Breinholt, C. Earl, A. R. Lemmon, E. M. Lemmon, L. Xiao, A. Y. Kawahara, Resolving relationships among the megadiverse butterflies and moths with a novel pipeline for anchored phylogenomics. *Syst. Biol.* **0**, 1–16 (2017).
22. D. L. Rabosky, E. E. Goldberg, FiSSE: A simple nonparametric test for the effects of a binary character on lineage diversification rates. *Evolution* **71**, 1432–1442 (2017).
23. D. Outomuro, F. Bokma, F. Johansson, Hind wing shape evolves faster than front wing shape in *Calopteryx* damselflies. *Evol. Biol.* **39**, 116–125 (2012).
24. B. Jantzen, T. Eisner, Hindwings are unnecessary for flight but essential for execution of normal evasive flight in Lepidoptera. *Proc. Natl. Acad. Sci. U.S.A.* **105**, 16636–16640 (2008).
25. S. A. Combes, D. E. Rundle, J. M. Iwasaki, J. D. Crall, Linking biomechanics and ecology through predator-prey interactions: Flight performance of dragonflies and their prey. *J. Exp. Biol.* **215**, 903–913 (2012).
26. A. J. Corcoran, W. E. Conner, How moths escape bats: Predicting outcomes of predator-prey interactions. *J. Exp. Biol.* **219**, 2704–2715 (2016).
27. M. K. Wourms, F. E. Wasserman, Butterfly wing markings are more advantageous during handling than during the initial strike of an avian predator. *Evolution* **39**, 845–851 (1985).
28. R. K. Robbins, The "false head" hypothesis : Predation and wing pattern variation of lycaenid butterflies. *Am. Nat.* **118**, 770–775 (1981).
29. A. Sourakov, Two heads are better than one: False head allows *Calycopis cecrops* (Lycaenidae) to escape predation by a jumping spider, *Phidippus pulcherrimus* (Salticidae). *J. Nat. Hist.* **47**, 1047–1054 (2013).
30. M. J. Scoble, *The Lepidoptera. Form, Function and Diversity* (Oxford Univ. Press, 1992).
31. A. Denzinger, H.-U. Schnitzler, Bat guilds, a concept to classify the highly diverse foraging and echolocation behaviors of microchiropteran bats. *Front. Physiol.* **4**, 164 (2013).
32. K. Hulgard, J. M. Ratcliffe, Sonar sound groups and increased terminal buzz duration reflect task complexity in hunting bats. *Sci. Rep.* **6**, 21500 (2016).
33. A. W. Shingleton, W. A. Frankino, T. Flatt, H. F. Nijhout, D. J. Emlen, Size and shape: The developmental regulation of static allometry in insects. *Bioessays* **29**, 536–548 (2007).
34. M. R. Evans, A. L. R. Thomas, The aerodynamic and mechanical effects of elongated tails in the scarlet-tufted malachite sunbird: Measuring the cost of a handicap. *Anim. Behav.* **43**, 337–347 (1992).

35. R. Norberg, Swallow tail streamer is a mechanical device for self deflection of tail leading edge, enhancing aerodynamic efficiency and flight manoeuvrability. *Proc. R. Soc. Lond. B Biol. Sci.* **257**, 227–233 (1994).
36. P. Chai, D. Millard, Flight and size constraints: Hovering performance of large hummingbirds under maximal loading. *J. Exp. Biol.* **200**, 2757–2763 (1997).
37. E. S. Morton, The function of multiple mating by female promethea moths, *Callosamia promethea* (Drury) (Lepidoptera:Saturniidae). *Am. Midl. Nat.* **162**, 7–18 (2009).
38. H. F. Nijhout, W. A. Smith, I. Schachar, S. Subramanian, A. Tobler, L. W. Grunert, The control of growth and differentiation of the wing imaginal disks of *Manduca sexta*. *Dev. Biol.* **302**, 569–576 (2007).
39. Y. Yovel, M. O. Franz, P. Stilz, H.-U. Schnitzler, Complex echo classification by echo-locating bats: A review. *J. Comp. Physiol. A Neuroethol. Sens. Neural Behav. Physiol.* **197**, 475–490 (2011).
40. J. Ylla, R. S. Peigler, A. Y. Kawahara, Cladistic analysis of moon moths using morphology, molecules, and behaviour: (Lepidoptera: Saturniidae). *SHILAP Revta. Lepid.* **33**, 299–317 (2005).
41. K. Arbuckle, M. P. Speed, Antipredator defenses predict diversification rates. *Proc. Natl. Acad. Sci. U.S.A.* **112**, 13597–13602 (2015).
42. V. Bonhomme, S. Picq, C. Gaucherel, J. Claude, Momocs: Outline analysis using R. *J. Stat. Softw.* **56**, 1–24 (2014).
43. H. Iwata, Y. Ukai, SHAPE: A computer program package for quantitative evaluation of biological shapes based on elliptic Fourier descriptors. *J. Hered.* **93**, 384–385 (2002).
44. V. Bonhomme, S. Prasad, C. Gaucherel, Intraspecific variability of pollen morphology as revealed by elliptic Fourier analysis. *Plant Syst. Evol.* **299**, 811–816 (2013).
45. D. H. Chitwood, Imitation, genetic lineages, and time influenced the morphological evolution of the violin. *PLOS ONE* **9**, e109229 (2014).
46. D. H. Chitwood, N. R. Sinha, Evolutionary and environmental forces sculpting leaf development. *Curr. Biol.* **26**, R297–R306 (2016).
47. J. C. Regier, M. C. Grant, C. C. Mitter, C. P. Cook, R. S. Peigler, R. Rougerie, Phylogenetic relationships of wild silkmoths (Lepidoptera: Saturniidae) inferred from four protein-coding nuclear genes. *Syst. Entomol.* **33**, 219–228 (2008).
48. A. R. Lemmon, S. A. Emme, E. M. Lemmon, Anchored hybrid enrichment for massively high-throughput phylogenomics. *Syst. Biol.* **61**, 727–744 (2012).
49. K. Katoh, D. M. Standley, MAFFT multiple sequence alignment software version 7: Improvements in performance and usability. *Mol. Biol. Evol.* **30**, 772–780 (2013).
50. P. Kück, G. C. Longo, FASconCAT-G: Extensive functions for multiple sequence alignment preparations concerning phylogenetic studies. *Front. Zool.* **11**, 81 (2014).
51. L.-T. Nguyen, H. A. Schmidt, A. von Haeseler, B. Q. Minh, IQ-TREE: A fast and effective stochastic algorithm for estimating maximum-likelihood phylogenies. *Mol. Biol. Evol.* **32**, 268–274 (2015).
52. E. Paradis, J. Claude, K. Strimmer, APE: Analyses of phylogenetics and evolution in R language. *Bioinformatics* **20**, 289–290 (2004).
53. E. Paradis, *Analysis of Phylogenetics and Evolution with R* (Springer Science and Business Media, 2011).
54. E. W. Goolsby, J. Bruggeman, C. Ané, Rphylopars: Fast multivariate phylogenetic comparative methods for missing data and within-species variation. *Methods Ecol. Evol.* **8**, 22–27 (2017).
55. L. J. Revell, Phylogenetic signal and linear regression on species data. *Methods Ecol. Evol.* **1**, 319–329 (2010).
56. J. Eberle, R. C. M. Warnock, D. Ahrens, Bayesian species delimitation in *Pleophylla* chafers (Coleoptera)—The importance of prior choice and morphology. *BMC Evol. Biol.* **16**, 94 (2016).
57. T. Ingram, D. L. Mahler, SURFACE: Detecting convergent evolution from comparative data by fitting Ornstein-Uhlenbeck models with stepwise Akaike information criterion. *Methods Ecol. Evol.* **4**, 416–425 (2013).
58. L. J. Revell, phytools: An R package for phylogenetic comparative biology (and other things). *Methods Ecol. Evol.* **3**, 217–223 (2012).
59. L. J. Revell, Two new graphical methods for mapping trait evolution on phylogenies. *Methods Ecol. Evol.* **4**, 754–759 (2013).
60. C. A. Schneider, W. S. Rasband, K. W. Eliceiri, NIH Image to ImageJ: 25 years of image analysis. *Nat. Methods* **9**, 671–675 (2012).
61. J. K. Kruschke, *Doing Bayesian Data Analysis, Second Edition: A Tutorial with R, JAGS, and Stan* (Academic Press, ed. 2, 2010).
62. M. Kéry, M. Schaub, *Bayesian Population Analysis using WinBUGS: A Hierarchical Perspective* (Elsevier, 2012).
63. C. J. W. McClure, B. W. Rolek, T. I. Hayes, C. D. Hayes, R. Thorstrom, M. Curti, D. L. Anderson, Successful enhancement of Ridgway's Hawk populations through recruitment of translocated birds. *Condor* **119**, 855–864 (2017).
64. M. Plummer, JAGS: A program for analysis of Bayesian graphical models using Gibbs sampling, in *Proceedings of the 3rd International Workshop on Distributed Statistical Computing*, K. Hornik, F. Leisch, A. Zeileis, Eds. (2003), vol. 124, pp. 1–10.
65. K. Kellner, jagsUI: A wrapper around "rjags" to streamline "JAGS" analyses (2016); https://CRAN.R-project.org/package=jagsUI.
66. R Core Team, R: A language and environment for statistical computing (2016).
67. A. Gelman, D. B. Rubin, Inference from iterative simulation using multiple sequences. *Stat. Sci.* **7**, 457–472 (1992).
68. T. L. Hedrick, Software techniques for two- and three-dimensional kinematic measurements of biological and biomimetic systems. *Bioinspir. Biomim.* **3**, 034001 (2008).
69. D. H. Theriault, N. W. Fuller, B. E. Jackson, E. Bluhm, D. Evangelista, Z. Wu, M. Betke, T. L. Hedrick, A protocol and calibration method for accurate multi-camera field videography. *J. Exp. Biol.* **217**, 1843–1848 (2014).
70. F. E. Harrell Jr., Package "Hmisc" (R Foundation Statistics and Computing, 2017).
71. D. R. Griffin, F. A. Webster, C. R. Michael, The echolocation of flying insects by bats. *Anim. Behav.* **8**, 141–154 (1960).
72. C. Geberl, S. Brinkløv, L. Wiegrebe, A. Surlykke, Fast sensory–motor reactions in echolocating bats to sudden changes during the final buzz and prey intercept. *Proc. Natl. Acad. Sci. U.S.A.* **112**, 4122–4127 (2015).
73. L. Jakobsen, A. Surlykke, Vespertilionid bats control the width of their biosonar sound beam dynamically during prey pursuit. *Proc. Natl. Acad. Sci. U.S.A.* **107**, 13930–13935 (2010).
74. J. M. Ratcliffe, C. P. H. Elemans, L. Jakobsen, A. Surlykke, How the bat got its buzz. *Biol. Lett.* **9**, 20121031 (2013).

Acknowledgments: We thank K. Miner and A. Lofthus for bat care and data analysis; University of Florida undergraduates N. Sewnath, S. McGiveron, D. Philoctete, and A. Mahadai for aiding with digitization of specimens; A. Baranowski for donating specimens; S. Combes, D. Mennitt, and B. Leavell for insightful discussion; and B. Conner for comments. **Funding:** This work was partly supported by NSF grants IOS-1121807 (to J.R.B.), IOS-1121739 (to A.Y.K.), DBI-1349345 (to A.Y.K.), DEB-1557007 (to A.Y.K.), and PRFB-1612862 (to C.A.H.); National Geographic Society grants CRE 9944-16 (to J.R.B.) and YEG 9965-16 (to J.J.R.); postdoctoral support from the Florida Museum of Natural History (to C.A.H.); and graduate research support from Boise State University and Sigma Xi Grants-in-Aid of Research (to J.J.R.). **Author contributions:** J.J.R. and J.R.B. designed behavioral experiments and wrote the first draft of the manuscript. J.J.R. collected behavioral data. J.J.R., C.J.W.M., B.A.C., and J.R.B. ran behavioral analyses. C.A.H. and A.Y.K. ran morphometric, phylogenomic, and comparative analyses. All authors contributed to the writing of the manuscript. **Competing interests:** The authors declare that they have no competing interests. **Data and materials availability:** All data needed to evaluate the conclusions in the paper are present in the paper, in the Supplementary Materials, and/or available on the Dryad Digital Repository (____). Additional data related to this paper may be requested from the authors.

Submitted 12 December 2017
Accepted 29 May 2018
Published 4 July 2018
10.1126/sciadv.aar7428

Citation: J. J. Rubin, C. A. Hamilton, C. J. W. McClure, B. A. Chadwell, A. Y. Kawahara, J. R. Barber, The evolution of anti-bat sensory illusions in moths. *Sci. Adv.* **4**, eaar7428 (2018).